

"normal" photoreaction of the porphyrin is suppressed. We have previously shown that tin(IV) tetraphenylporphyrin dichloride can function in a solution-phase photoelectrochemical process with the same amines as reductants; here, however, rapid conversion of the porphyrin to a partially reduced species occurs, severely limiting the stability and steady-state current of the cell.<sup>55</sup> The most significant aspects of this study is the clear delineation of the effect of thickness of the multilayer and solute penetration on the three-way cooperative process. Thus, we find that for relatively hydrophobic solutes such as triethylamine or *N,N*-dimethylaniline, which readily penetrate the multilayers, there is an increase in the photocurrent up to ca. nine layers; at the same time there is considerable retardation of the "normal" photoreaction for these solutes with up to at least seven layers of porphyrin. Since the layer thickness should be on the order of 30 Å, the fact that quenching is observed suggests that the reactive porphyrin intermediate intercepted in eq 10 or 11 can migrate

(55) Chandrasekaran, K.; Whitten, D. G. *J. Am. Chem. Soc.* **1980**, *102*, 5119.

over distances in the range 210–270 Å. Experiments are currently underway to determine if this distance can be adjusted by the addition of cosurfactants including ones with extensive unsaturation or other redox active groups.

**Acknowledgment.** We thank the National Science Foundation (Grant No. CHE 78723126) for initial support of these studies and the Department of Energy (Contract DE-A505-81ER10815.A00) for present support. The photochemical ESR studies were carried out at the CNRS laboratory, Gif-sur-Yvette, France, through a NATO supported collaboration, and the laser-flash measurements were made at the EPFL-Ecublens Lausanne, Switzerland. We are very grateful to Mrs. Marjorie Richter for her technical assistance, and to Professor R. W. Murray for suggestions concerning the photoelectrochemical studies.

**Registry No.** SnO<sub>2</sub>, 18282-10-5; PtO<sub>2</sub>, 1314-15-4; SnPF<sub>6</sub>·THA·Cl<sub>2</sub>, 83152-03-8; O<sub>2</sub>, 7782-44-7; PMA, 121-69-7; DIPEA, 7087-68-5; HQ, 123-31-9; TEA, 121-44-8; PdPF<sub>6</sub>·THA, 83152-04-9; platinum, 7440-06-4; *N,N*-dimethyl-*p*-nitrosoaniline, 138-89-6; imidazole, 288-32-4; *p*-dimethoxybenzene, 150-78-7.

## Direct Measurement of the Chemical Shift Anisotropy of Thallium-205 Using the Matrix Isolation Technique. The Tl/K/NO<sub>3</sub> System

Kenneth R. Metz and James F. Hinton\*

Contribution from the Department of Chemistry, University of Arkansas, Fayetteville, Arkansas 72701. Received March 17, 1982

**Abstract:** Solid-state NMR spectra of <sup>203</sup>Tl and <sup>205</sup>Tl in pure TlNO<sub>3</sub> and mixtures of TlNO<sub>3</sub> with various monovalent metal nitrates have been determined in order to evaluate the magnitude of the thallium shielding anisotropy in ionic environments. The room-temperature line width of pure TlNO<sub>3</sub> arises mainly from indirect scalar exchange interactions and chemical shielding anisotropy at 2.114 T. Samples prepared from mixed melts of TlNO<sub>3</sub> with LiNO<sub>3</sub>, NaNO<sub>3</sub>, or AgNO<sub>3</sub> show <sup>205</sup>Tl spectra identical with those of pure TlNO<sub>3</sub> from 25 to 160 °C, suggesting ion segregation in the solid. Dramatic narrowing of the resonance line in Tl/K/NO<sub>3</sub> mixtures allows observation of NMR powder patterns which strongly reflect the microscopic structure of KNO<sub>3</sub>. At room temperature, the shift is about -300 ppm, suggesting high ionic character, and  $\sigma_{\perp} - \sigma_{\parallel}$  is about 50 ppm. Above the KNO<sub>3</sub> II → I phase transition at 128 °C, the shielding is nonaxially symmetric with  $\sigma_{33} - \sigma_{11}$  of about 90 ppm. The large  $\Delta\delta$  values exhibited by thallium in this ionic system suggest the potential for enormous shielding anisotropies in covalent thallium compounds.

Among the areas of vigorous current research in NMR spectroscopy is the study of nuclei undergoing restricted motion. Although the practical difficulties associated with these studies can be formidable, the efforts of a growing number of laboratories have produced a significant body of knowledge concerning the NMR properties of spins in rigid or semirigid systems. This is especially true of some of the "classical" nuclides (e.g., <sup>1</sup>H and <sup>13</sup>C) but is much less true of many of the other observable elements in the periodic table.

One of the most interesting among this latter group is thallium. Two common isotopes exist, both with spin 1/2. The most abundant (70.5%) is <sup>205</sup>Tl with a magnetogyric ratio of  $15.44 \times 10^7$  rad s<sup>-1</sup> T<sup>-1</sup>, while <sup>203</sup>Tl makes up the remaining 29.5% and possesses a magnetogyric ratio of  $15.29 \times 10^7$  rad s<sup>-1</sup> T<sup>-1</sup>. <sup>205</sup>Tl has an excellent NMR receptivity (0.1355 relative to <sup>1</sup>H) and a chemical shift range approaching 7500 ppm, making it an attractive probe for NMR investigations of chemical systems.

It is clear that a better understanding of the NMR shielding tensor properties of thallium will enhance its value as a probe, even in solution. This has been demonstrated, for example, by the recent finding<sup>1</sup> that the <sup>205</sup>Tl shielding anisotropy of the solid

Tl(I)-valinomycin complex is actually much smaller than predicted<sup>2</sup> from spin-lattice relaxation times in solution. The shift of this ionic complex nevertheless exhibits a surprisingly large anisotropy of 150 ppm. Few other thallium chemical shift anisotropies have been reported,<sup>3-6</sup> and highly ionic systems such as the one investigated here have been particularly neglected.

Several methods may be used to characterize the NMR shielding tensor. One approach involves measurement of the orientation dependence of the chemical shift of a single crystal, and all nine shielding tensor elements may be determined by this technique. If only a powder is available, the NMR spectrum may exhibit singularities at chemical shifts corresponding to values of

(1) Hinton, J. F.; Metz, K. R.; Millett, F. S. *J. Magn. Reson.* **1981**, *44*, 217.

(2) Briggs, R. W.; Hinton, J. F. *J. Magn. Reson.* **1978**, *32*, 155.

(3) Vaughan, R. W.; Anderson, D. H. *J. Chem. Phys.* **1970**, *52*, 5287.

(4) Panek, L. W.; Exarhos, G. J.; Bray, P. J.; Risen, W. M. *J. Non-Cryst. Solids* **1977**, *24*, 51.

(5) Bloembergen, N.; Rowland, T. J. *Phys. Rev.* **1955**, *97*, 1679.

(6) Matsuo, T.; Sugisaki, M.; Suga, H.; Seki, S. *Bull. Chem. Soc. Jpn.* **1969**, *42*, 1271.

the three principal elements of the shielding tensor. In pure thallium salts, however, line broadening which results mainly from indirect  $^{203}\text{Tl}$ - $^{205}\text{Tl}$  spin-spin interactions<sup>7</sup> nearly always obscures the powder pattern singularities. One straightforward method for eliminating these indirect interactions is dilution in a matrix which is magnetically inert. Solid potassium(I) nitrate approximates such a matrix. Both of the potassium isotopes present have small magnetogyric ratios ( $1.2 \times 10^7$  and  $0.7 \times 10^7$  rad s<sup>-1</sup> T<sup>-1</sup> for  $^{39}\text{K}$  and  $^{41}\text{K}$ , respectively) and should not interact strongly with nearby thallium nuclei. Of the other nuclides,  $^{17}\text{O}$  is present in only very small quantities (0.037% natural abundance) and  $^{14}\text{N}$ , which comprises 99.63% of the total nitrogen, possesses a small magnetogyric ratio ( $1.93 \times 10^7$  rad s<sup>-1</sup> T<sup>-1</sup>).

Potassium(I) nitrate exhibits two stable phases at atmospheric pressure, and both of these have been studied extensively by X-ray,<sup>8-16</sup> vibrational,<sup>17-20</sup> optical,<sup>8,21</sup> magnetic,<sup>22,23</sup> electrical,<sup>8,24,25</sup> and thermal<sup>26</sup> techniques. The similarities between the ionic radii of thallium (0.140 nm) and potassium (0.133 nm) should allow Tl(I) ions to occupy K(I) lattice sites with relatively little distortion. It is thus possible to correlate observed thallium shielding properties with the known microscopic structure of the matrix and thereby characterize the factors which affect the shielding tensor.

### Experimental Section

Thallium(I) nitrate was Fisher purified grade which was recrystallized repeatedly from distilled, deionized water. All other metal nitrates were of ACS Reagent quality. Mixtures were prepared by weighing the dry salts into borosilicate glass bulbs under dry nitrogen. The bulbs were heated, again under dry nitrogen, until melting occurred, and heat was applied intermittently for, typically, 2 min during mixing. Excessive heat was carefully avoided due to the low decomposition temperatures of the metal nitrates. After cooling to room temperature, the mixtures were finely crushed and transferred to Wilmad 505-PS 5-mm (o.d.) NMR tubes, and the samples were then sealed under approximately 0.8 atm of dry nitrogen.

All  $^{205}\text{Tl}$  NMR spectra were obtained by using a modified Bruker HFX-90 spectrometer operating in the pulsed FT mode at a magnetic field strength of 2.114 T. The  $^{205}\text{Tl}$  transmitter, single-coil probe insert, and broad-band preamp used were constructed in this laboratory. When an ENI 3100L broad-band rf power amplifier was used, a 90° pulse could be applied in about 15 s ( $B_1 = 7 \times 10^{-4}$  T). Data were digitized by using a Nicolet 2090-III digital oscilloscope and, by means of an interface constructed in this laboratory,<sup>27</sup> transferred to a Nicolet NMR-80 computer system for averaging and reduction. Sample temperatures were controlled by a Bruker BST 100/700 controller.

Spectra were acquired by using 10–35° pulses, and 10–20 s was allowed between pulses for relaxation. Longer delays were not found to alter the spectra. The rf phase was shifted in 180° increments to cancel coherent noise. A continuous-wave field-frequency lock was maintained at 90 MHz by using the methyl proton signal from a capillary of mesitylene contained inside each sample tube. The lock rf was gated off during acquisition of the free induction decay. Correction of the  $^{205}\text{Tl}$  shifts to a Me<sub>4</sub>Si lock does not produce significantly different values from those found directly using mesitylene, so corrections have not been ap-

(7) Hinton, J. F.; Metz, K. R.; Briggs, R. W. *Annu. Rep. NMR Spectrosc.*, in press.

(8) McLaren, A. C.; *Rev. Pure Appl. Chem.* **1962**, *12*, 54.

(9) Bragg, W. L. *Proc. R. Soc. London, Ser. A* **1924**, *105*, 16.

(10) Edwards, D. A. Z. *Kristallogr.* **1931**, *A80*, 154.

(11) Kracek, F. C.; Barth, T. F. W.; Ksanda, C. J. *Phys. Rev.* **1932**, *40*, 1034.

(12) Leonhardt, J.; Borchert, W. *Naturwissenschaften* **1936**, *24*, 412.

(13) Finbak, C.; Hassel, O. Z. *Phys. Chem., Abt. B* **1937**, *37*, 75.

(14) Barth, T. F. W. Z. *Phys. Chem., Abt. B* **1939**, *43*, 448.

(15) Kennedy, S. W.; Ubbelohde, A. R.; Woodward, I. *Proc. R. Soc. London, Ser. A* **1953**, *219*, 303.

(16) Fischmeister, H. F.; *J. Inorg. Nucl. Chem.* **1956**, *3*, 182.

(17) Vratny, F. *Appl. Spectrosc.* **1959**, *13*, 59.

(18) Ferraro, J. R. J. *Mol. Spectrosc.* **1960**, *4*, 99.

(19) Wait, S. C.; Ward, A. T.; Janz, G. J. *J. Chem. Phys.* **1966**, *45*, 133.

(20) Brooker, M. H.; Irish, D. E. *Can. J. Chem.* **1970**, *48*, 1183.

(21) Rhodes, E.; Ubbelohde, A. R. *Proc. R. Soc. London, Ser. A* **1959**, *251*, 156.

(22) Schulze, G. E. R. Z. *Phys. Chem., Abt. B* **1938**, *40*, 308.

(23) Cini, R.; Ferroni, E.; Cocchi, M. *Ann. Chim. (Rome)* **1957**, *47*, 841.

(24) Jaffray, J. C. R. *Hebd. Acad. Sci. Seances* **1950**, *230*, 525.

(25) Swada, S.; Nomura, S.; Fujii, S. J. *Phys. Soc. Jpn.* **1958**, *13*, 1549.

(26) Kracek, F. C. *J. Phys. Chem.* **1930**, *34*, 225.

(27) Metz, K. R.; Hinton, J. F. J. *Magn. Reson.* **1981**, *45*, 229.

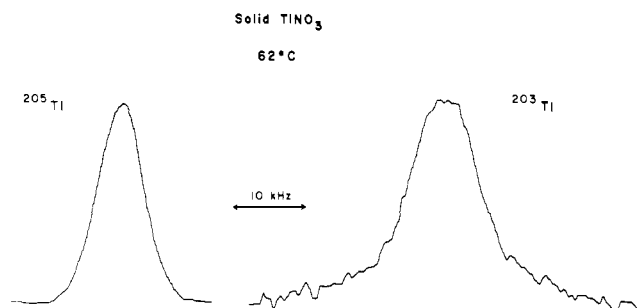


Figure 1.  $^{203}\text{Tl}$  and  $^{205}\text{Tl}$  NMR spectra of pure solid thallium(I) nitrate at 2.114 T and 62 °C. Line widths are independent of temperature below the  $\text{TlNO}_3$  phase transition at 79 °C. Resonance frequencies are  $51.4025 \pm 0.0005$  ( $^{203}\text{Tl}$ ) and  $51.9084 \pm 0.0003$  ( $^{205}\text{Tl}$ ) MHz.

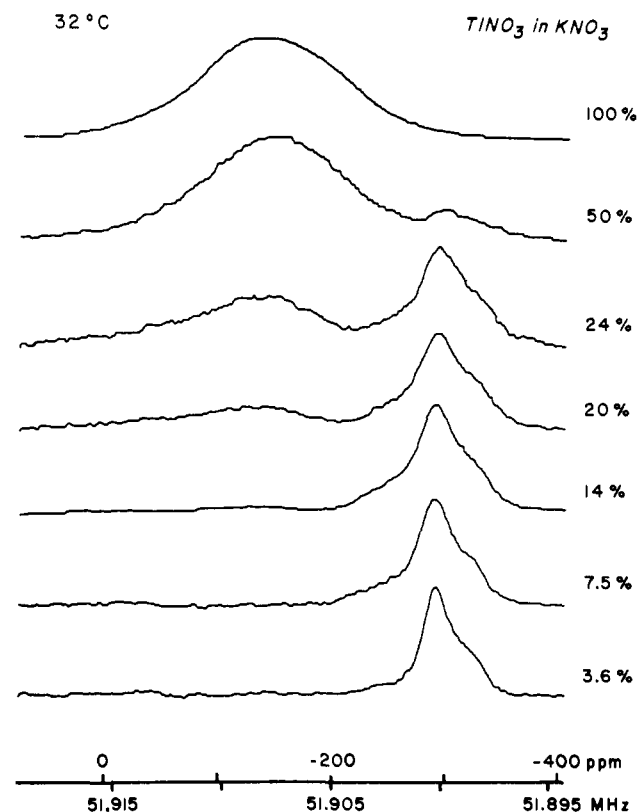


Figure 2.  $^{205}\text{Tl}$  NMR spectra of Tl/K/ $\text{NO}_3$  mixtures (including pure  $\text{TlNO}_3$  for comparison).

plied. Shifts are quoted relative to infinitely dilute aqueous  $\text{TlNO}_3$  (51,915, 450 Hz at this  $B_0$ ), and upfield shifts have been assigned negative values as usual.

Shielding tensor elements and line widths were extracted by fitting the experimental spectra with theoretical patterns calculated from standard equations.<sup>28,29</sup> An interactive BASIC program POWDER was written for this purpose.

### Results and Discussion

**The Tl/K/ $\text{NO}_3$  System.** The  $^{203}\text{Tl}$  and  $^{205}\text{Tl}$  NMR spectra of pure thallium(I) nitrate powder are shown in Figure 1. It is obvious that spectral fine structure due to underlying chemical shift anisotropy is effectively obscured in this salt. The question of shielding anisotropy in thallium(I) nitrate has not previously been addressed, but there is strong evidence for its existence. The  $^{205}\text{Tl}$  line width of  $7.1 \pm 0.4$  kHz found at the present field strength (2.114 T) exceeds the value of 5.2 kHz determined<sup>30</sup> at 0.855 T, suggesting contributions from shielding anisotropy. Furthermore, we have found the  $^{205}\text{Tl}$  line width in a single crystal to be only

(28) Bloembergen, N.; Rowland, T. J. *Acta Metall.* **1953**, *1*, 731.

(29) Haeberlen, U. In "Advances in Magnetic Resonance"; Waugh, J. S., Ed.; Academic Press: New York, 1976; Supplement 1.

(30) Kolditz, L.; Wahnner, E. Z. *Anorg. Allg. Chem.* **1973**, *400*, 161.

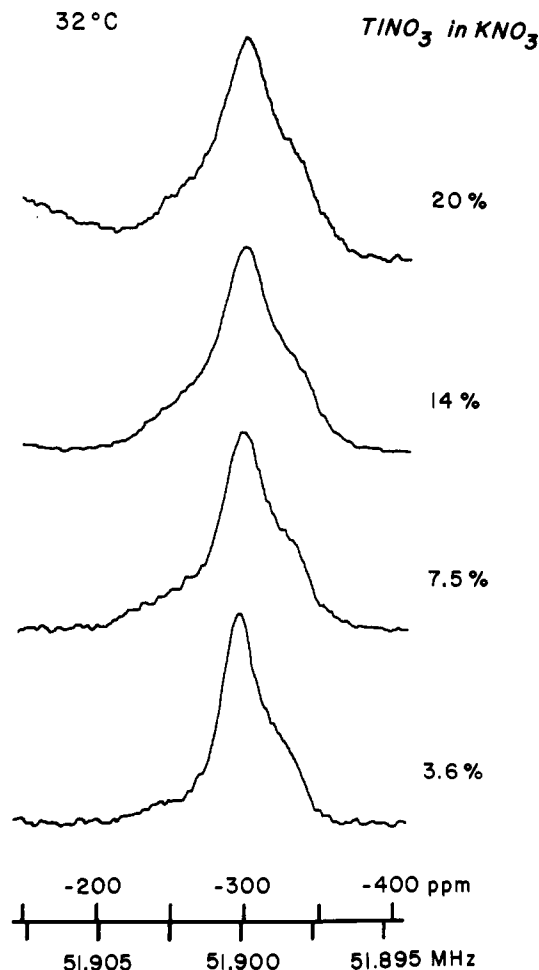


Figure 3.  $^{205}\text{Tl}$  NMR powder line shapes for Tl(I) isolated in a  $\text{KNO}_3$  matrix.

$3.8 \pm 0.5$  KHz and independent of crystal orientation relative to the direction of the applied field within experimental error. Chemical shift anisotropy must then account for approximately 3.3 kHz of the 7.1-kHz total powder line width at this field strength. The lack of an orientation dependence suggests that dipolar line-width contributions are small, although the same effect would be observed if dipolar couplings were fortuitously of equal magnitudes and opposite signs.

The  $^{203}\text{Tl}$  and  $^{205}\text{Tl}$  line widths of Figure 1 are quite different, demonstrating the importance of  $^{203}\text{Tl}$ - $^{205}\text{Tl}$  scalar exchange interactions in thallium(I) nitrate. Since exchange broadening only arises from interactions between different isotopes,<sup>5</sup> the broader line is that of  $^{203}\text{Tl}$  which, at 29.5% natural abundance, is surrounded primarily by unlike  $^{205}\text{Tl}$ . Scalar exchange has previously<sup>31-33</sup> been found to contribute to the line width in this salt.

In view of the effect of exchange on the thallium(I) nitrate powder line width, dilution in a magnetically inert matrix should lead to narrowing of the thallium resonance line. Figure 2 shows  $^{205}\text{Tl}$  NMR spectra of various mixtures of thallium(I) nitrate with potassium(I) nitrate. It is immediately obvious that isolated regions of relatively pure  $\text{TlNO}_3$  form upon cooling melts containing high thallium concentrations. However, the dilute mixtures yield the predicted narrower lines with chemical shifts characteristic of  $^{205}\text{Tl}$  in quite a different environment—that of the  $\text{KNO}_3$  matrix. The change in  $^{205}\text{Tl}$  chemical shift evident in Figure 2 is not surprising in view of differences in the crystal structures of  $\text{TlNO}_3$  and  $\text{KNO}_3$ . Although both form orthorhombic crystals

Table I. Line Shape Parameters at 32 °C for Various Concentrations of  $\text{TlNO}_3$  in  $\text{KNO}_3$ <sup>a</sup>

$[\text{TlNO}_3]$ , mol %	$\sigma_{\perp}$ , MHz/ppm	$\sigma_{\parallel}$ , MHz/ppm	$\Delta\sigma$ , Hz/ppm	line width, Hz
3.6	51.900 62/-285	51.898 04/-335	2580/50	900
7.5	51.900 60/-285	51.897 72/-341	2880/56	1070
14	51.900 52/-287	51.897 58/-344	2950/57	1280
20	51.900 46/-289	51.897 46/-346	3000/58	1360

<sup>a</sup> Estimated uncertainties are as follows:  $\pm 0.4$  mol %;  $\pm 50$  Hz and  $\pm 1$  ppm ( $\sigma_{\perp}$ );  $\pm 100$  Hz and  $\pm 2$  ppm ( $\sigma_{\parallel}$ );  $\pm 150$  Hz and  $\pm 3$  ppm ( $\Delta\sigma$ );  $\pm 100$  Hz (line width).

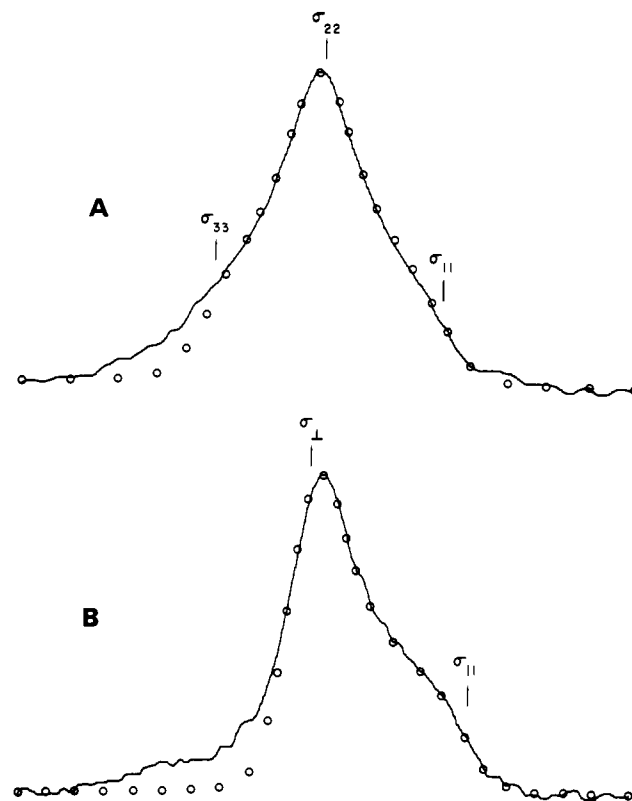


Figure 4. Typical theoretical fits to  $^{205}\text{Tl}$  powder patterns from Tl/K/ $\text{NO}_3$ . Solid lines are experimental spectra and open circles are theoretical points: (A) 7.5 mol % at 120 °C; (B) 3.6 mol % at 32 °C.

at room temperature,  $\text{KNO}_3$  (form II, below 128 °C) takes the aragonite structure with four formula units per unit cell<sup>10,12,14-16</sup> while  $\text{TlNO}_3$  (form III, below 79 °C) has space group  $Pbnm$  or  $Pbn2_1$  with eight formula units per unit cell.<sup>34-36</sup>

Careful examination of the signal from  $^{205}\text{Tl}$  dispersed in the  $\text{KNO}_3$  matrix (Figure 3) shows that additional line narrowing results from increasing dilution. This occurs to such an extent that the chemical shift anisotropy is now clearly evident and is of the axially symmetric type. In addition to the main line centered at about -300 ppm, a small component at approximately -250 ppm exists whose relative concentration decreases with greater dilution. At a molar concentration of 3.6% (a K:Tl ratio of about 27:1), this component has nearly disappeared. The main pattern at -300 ppm is almost certainly due to well-isolated  $^{205}\text{Tl}$  while the signal intermediate between this and pure  $\text{TlNO}_3$  results from regions of higher local concentrations of thallium. The  $^{203}\text{Tl}$  spectrum of the 7.5 mol % sample is identical with the  $^{205}\text{Tl}$  spectrum within experimental error. This provides further evidence for high isolation of thallium nuclei in the matrix, since exchange broadening would be expected to result from interactions within thallium clusters.

(31) Freeman, R.; Gasser, R. P. H.; Richards, R. E. *Mol. Phys.* **1959**, *2*, 301.

(32) Avogadro, A.; Villa, M.; Chiodelli, G. *Gazz. Chim. Ital.* **1976**, *106*, 413.

(33) Villa, M.; Avogadro, A. *Phys. Status Solidi B* **1976**, *75*, 179.

(34) Ferrari, A.; Cavalca, L. *Gazz. Chim. Ital.* **1950**, *80*, 199.

(35) Hinde, R. M.; Kellett, E. A. *Acta Crystallogr.* **1957**, *10*, 383.

(36) Brown, R. N.; McLaren, A. C. *Acta Crystallogr.* **1962**, *15*, 977.

Table II.  $^{205}\text{Tl}$  Line Shape Parameters for 7.5 mol %  $\text{TlNO}_3$  in  $\text{KNO}_3$  at Various Temperatures<sup>a</sup>

temp, °C	$\sigma_{11}$ , MHz/ppm	$\sigma_{22}$ , MHz/ppm	$\sigma_{33}$ , MHz/ppm	line width, Hz
-38	51.896 65/-362	51.899 64/-304	<i>b</i>	1250
32	51.897 72/-341	51.900 60/-286	<i>b</i>	1070
69	51.898 27/-331	51.900 90/-280	<i>b</i>	1140
84	51.898 40/-328	51.901 12/-276	<i>b</i>	1080
102	51.898 46/-327	51.901 25/-273	<i>b</i>	1220
120	51.902 16/-256	51.904 49/-211	51.906 60/-170	1110
137	51.902 32/-253	51.904 65/-208	51.906 97/-163	1110
156	51.902 69/-246	51.904 85/-204	51.907 40/-155	1050

<sup>a</sup> Estimated uncertainties are as follows:  $\pm 2$  °C;  $\pm 150$  Hz and  $\pm 3$  ppm ( $\sigma_{11}$ );  $\pm 100$  Hz and  $\pm 2$  ppm ( $\sigma_{22}$ );  $\pm 200$  Hz and  $\pm 4$  ppm ( $\sigma_{33}$ );  $\pm 100$  Hz (line width). <sup>b</sup> Axial symmetry in the low-temperature form yields  $\sigma_{11} = \sigma_{22}$  and  $\sigma_{33} = \sigma_{\perp}$ .

Theoretical line-shape analysis of the powder patterns of Figure 3 yields the shielding tensor elements and line widths given in Table I. In all cases, reasonably good fits were obtained by using Gaussian line shapes (Figure 4). The line narrowing at greater dilutions qualitatively apparent in Figure 3 is quantitatively verified in the table. The tensor elements also exhibit concentration-dependent trends, with greater changes in  $\sigma_{\parallel}$  than in  $\sigma_{\perp}$ . McLaren<sup>8</sup> has envisioned form II  $\text{KNO}_3$  as containing long "rods" which run parallel to the *c* axis of the crystal. Each rod carried either  $\text{K}^+$  or  $\text{NO}_3^-$  ions, but not both. This model suggests an association between  $\sigma_{\parallel}$  and the axis along a rod of cations, with  $\sigma_{\perp}$  corresponding to interactions between  $^{205}\text{Tl}$  and  $\text{NO}_3^-$  ions in transverse directions perpendicular to this axis. The low-field shift of  $\sigma_{\perp}$  relative to  $\sigma_{\parallel}$  is also consistent with this orientation since  $\sigma_{\parallel}$  would then represent interactions with electron-deficient cations while interactions with electron-rich anions would dominate  $\sigma_{\perp}$ . The similar crystalline ionic radii of  $\text{K(I)}$  and  $\text{Tl(I)}$  probably allow  $\text{Tl(I)}$  ions to occupy  $\text{K(I)}$  sites without extensive lattice distortion, although the concentration dependence of the values of the tensor elements suggests that some distortion occurs. Such distortion need not be isotropic, as indicated by the somewhat different effects observed for  $\sigma_{\parallel}$  and  $\sigma_{\perp}$ .

**Temperature Dependence of Shieldings.** At 128 °C, pure form II  $\text{KNO}_3$  undergoes a phase transition to trigonal form I having the calcite structure and containing 12 formula units per unit cell.<sup>11-16</sup> In terms of the crystal model discussed above, each "rod" of the calcite structure simultaneously carries both cations and  $\text{NO}_3^-$  ions in an alternating sequence parallel to the *c* axis. Considerable lateral cation or anion movement must accompany the transition from form II to form I, and such a change in the host matrix structure would be expected to significantly alter the  $^{205}\text{Tl}$  shielding. This is indeed the case, as shown by Figure 5. The abrupt shift of the  $^{205}\text{Tl}$  resonance to lower field above the depressed transition temperature (ca. 110 °C) suggests closer crystal packing and correspondingly stronger electronic interactions with the cation. This interpretation is consistent with the preference of large cations for the more open aragonite structure and of small cations for the more closely packed calcite structure present in high-temperature form I  $\text{KNO}_3$ .<sup>8</sup>

Figure 5 also indicates a fundamental difference in symmetry about the cation in the two forms. While axially symmetric cations characterize the low-temperature form, the line shape in the high-temperature form may be fitted very well by using three distinct tensor elements (Figure 4). As at lower temperatures, a small peak overlaps the low-field edge of the main pattern and probably arises from regions of high local  $^{205}\text{Tl}$  concentration.

Best-fit  $^{205}\text{Tl}$  shielding tensor elements and line widths at various temperatures appear in Table II. A somewhat surprising result is that the line widths are essentially independent of temperature throughout the range studied. A large increase in the dc conductance of pure  $\text{KNO}_3$  at the form II  $\rightarrow$  form I transition has been cited as evidence for positional disorder in form I.<sup>8,24</sup> Yet, the line widths found for  $^{205}\text{Tl}$  contained in form I fail to provide the slightest indication of the postulated disorder. Several reasons

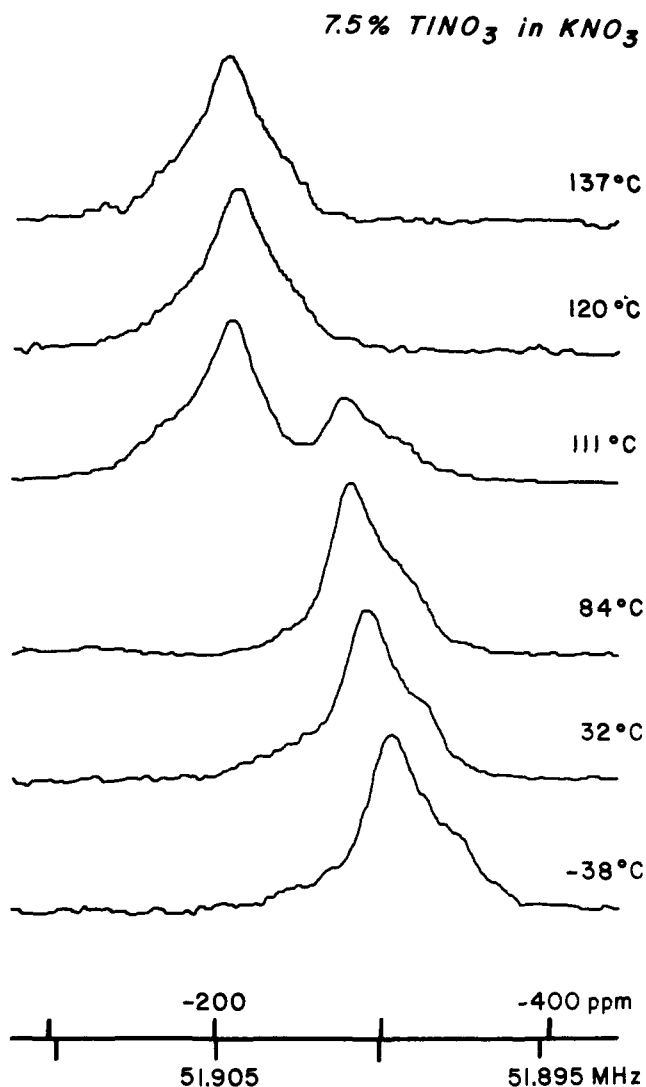


Figure 5.  $^{205}\text{Tl}$  NMR spectra of the  $\text{Tl/K/NO}_3$  system at various temperatures.

for this may be considered. It might be suggested that the  $^{205}\text{Tl}$  resonance line width is simply insensitive to motion in this system. Yet, the line exhibits dramatic narrowing at a similar disordering phase transition in pure  $\text{TlNO}_3$ , as discussed below. Possibly the increased conductance is electronic in nature and not positional, or  $\text{NO}_3^-$  may be the mobile ion instead of  $\text{K(I)}$ . Neither of these possibilities seems intuitively reasonable and, in either case, an effect on the  $^{205}\text{Tl}$  line width would be anticipated. In view of the smaller ionic radius of  $\text{K(I)}$  compared with that of  $\text{Tl(I)}$ , it could be argued that  $\text{K(I)}$  becomes mobile at the phase transition while bulkier  $\text{Tl(I)}$  remains bound. This is feasible, but it is still very surprising that the transition has no measurable effect on the  $^{205}\text{Tl}$  line width.

With increasing temperature, ions in a crystal lattice undergo greater vibrational motion. As the temperature increases from 128 to 335 °C, crystals of form I  $\text{KNO}_3$  exhibit a 6.8% expansion along the *c* axis but no change in directions perpendicular to this. Since the *c* axis parallel to the  $\text{NO}_3^-$  threefold rotation axes in form I, vibration by nitrate in this direction has been suggested.<sup>16</sup> It is reasonable to expect that transient vibrational distortions of  $\text{Tl(I)}$  should alter the  $^{205}\text{Tl}$  shielding, and this argument has been used previously to explain linear downfield shifts exhibited by a variety of thallium salts with increasing temperatures.<sup>37</sup> If local vibrational distortions are anisotropic, as in form I  $\text{KNO}_3$ , then the effect on the chemical shift should also be anisotropic. Figure 6 contains plots of  $^{205}\text{Tl}$  chemical shift against temperature for

(37) Hafner, S.; Nachtrieb, N. H. *J. Chem. Phys.* 1964, 40, 2891.

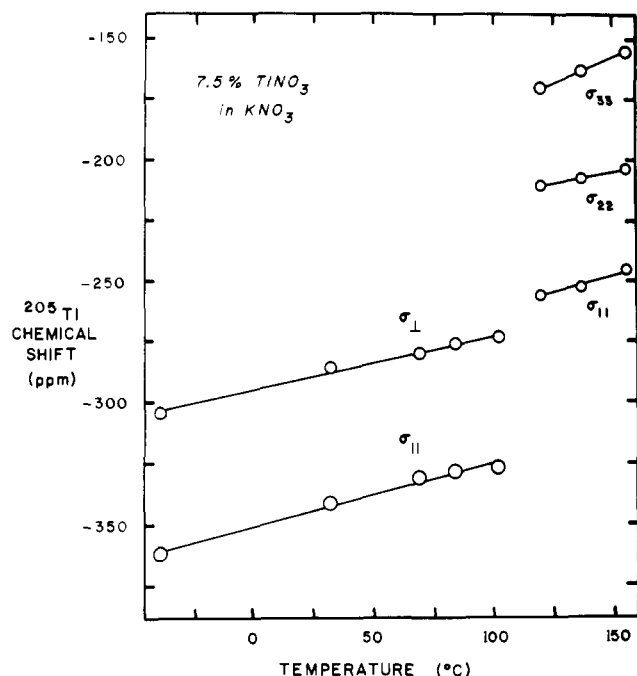


Figure 6. Temperature dependence of  $^{205}\text{Tl}$  shielding tensor elements of 7.5 mol %  $\text{TiNO}_3$  in  $\text{KNO}_3$ .

the tensor elements of Table II. All of the elements show essentially the same temperature dependence ( $0.24 \pm 0.05$  ppm  $\text{deg}^{-1}$ ) except for  $\sigma_{33}$  ( $0.43$  ppm  $\text{deg}^{-1}$ ), which suggests that  $\sigma_{33}$  lies parallel or nearly parallel to the  $c$  axis of form I. If  $\sigma_{\parallel}$  lies parallel to the  $c$  axis of form II, as previously discussed, then a downfield shift of some 150 ppm occurs upon replacement of cations above and below  $^{205}\text{Tl}$  with nitrate anions. Form II  $\sigma_{\perp}$  also splits into  $\sigma_{11}$  and  $\sigma_{22}$  in form I, as the lateral environment containing only  $\text{NO}_3^-$  groups in form II acquires cations as well in form I. The assignment of shielding tensor elements to molecular axes should always be recognized as uncertain in powders, however, so these assignments must be considered tentative.

**Other Host Lattices.** In addition to  $\text{KNO}_3$ , several other metal nitrates were chosen for use as  $\text{TiNO}_3$  hosts. Nitrates of lithium and sodium were chosen because they possess the calcite crystal structure at room temperature,<sup>16,38,39</sup> unlike  $\text{KNO}_3$  which takes this structure only in high-temperature form I. Silver nitrate was also used, since it has been reported to have a unique crystal structure.<sup>40</sup> The small magnetogyric ratio ( $-1.24 \times 10^7$  rad  $\text{T}^{-1} \text{s}^{-1}$ ) of  $^{101}\text{Ag}$  and its lack of a quadrupole moment were also advantageous. Interestingly, the  $^{205}\text{Tl}$  chemical shifts of  $\text{TiNO}_3$  mixtures with each of these salts were found to be virtually identical with the shift of pure  $\text{TiNO}_3$ . In addition, the  $^{205}\text{Tl}$  line widths obtained from these mixtures were very similar to those of pure  $\text{TiNO}_3$  (Figure 7). Distinct phase transitions are evident in the data of Figure 7, and, allowing for transition temperature depressions due to mixing, they correspond well with known transitions of pure  $\text{TiNO}_3$  at 79 and 144  $^\circ\text{C}$ . The transition at 144  $^\circ\text{C}$  has been attributed<sup>36</sup> to high Tl(I) mobility in this salt. In contrast, lithium and sodium nitrates are believed to be free of phase transitions to well above 200  $^\circ\text{C}$ , while silver nitrate undergoes a transition from orthorhombic form II to trigonal form I at about 160  $^\circ\text{C}$ .<sup>8</sup>

In view of the significant differences between the crystal structures of  $\text{TiNO}_3$  and the salts above, it seems most unlikely

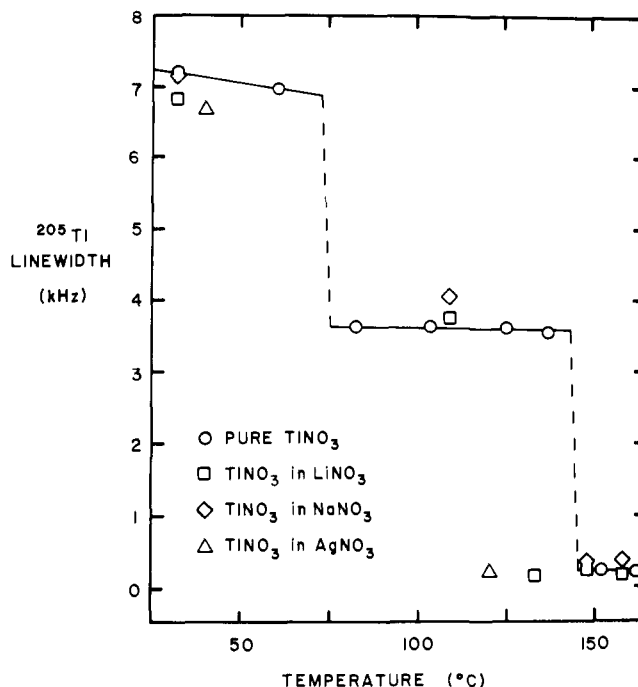


Figure 7.  $^{205}\text{Tl}$  NMR line width vs. temperature for pure  $\text{TiNO}_3$  and its mixtures with  $\text{LiNO}_3$ ,  $\text{NaNO}_3$ , and  $\text{AgNO}_3$  at 2.114 T.

that dilute molecular mixtures would exhibit chemical shifts identical with that of pure  $\text{TiNO}_3$ . The presence of phase transitions where none are known for the host salts is also inconsistent with the formation of intimate microscopic mixtures. It is therefore concluded that, upon rapid cooling of these melts, such mixtures do not form and the observed NMR properties are due to unmixed  $\text{TiNO}_3$ .

True ions, by their very nature, exhibit only weak electronic interactions with their surroundings. Since large differences in shielding tensor elements cannot exist in the absence of electronic interactions, the degree of ionic character limits the amount of chemical shift anisotropy which may be observed. Thus, comparatively small shielding anisotropies may be anticipated for highly ionic systems, while the potential exists for much greater anisotropies when stronger interactions occur. There can be little doubt of the highly ionic nature of  $^{205}\text{Tl}$  in pure  $\text{TiNO}_3$  since its resonance line lies some 135 ppm upfield from that of aqueous  $^{205}\text{Tl(I)}$ . The covalency of this salt has, in fact, been estimated at only 0.6%.<sup>37</sup> The chemical shift of about -300 ppm suggests even greater ionic character for Tl(I) isolated in the  $\text{KNO}_3$  matrix or perhaps it is associated with the effect of small symmetry changes on the orbital angular momentum about thallium. Yet, at high temperatures even this very ionic  $^{205}\text{Tl(I)}$  exhibits a remarkable chemical shift anisotropy of 91 ppm! The known  $^{205}\text{Tl}$  chemical shift range extends some 5600 ppm downfield of the aqueous  $^{205}\text{Tl(I)}$  reference and includes a number of rather covalent systems. For example, the shift of solid  $\text{Tl}_2\text{O}_3$  is reported<sup>5</sup> to be +5500 ppm, and its shielding anisotropy has been estimated at 1870 ppm. In view of the large shielding anisotropies exhibited by thallium even in ionic environments, it seems reasonable to predict enormous values for covalent species such as dialkylthallium(I) or trialkylthallium.

**Acknowledgment.** We acknowledge Mr. Kenneth H. McElveen for electronics assistance and Dr. Bernie Gerstein of the Department of Energy Ames Laboratory, Iowa State University, for useful advice and discussions. This research was supported by the National Science Foundation through grant PCM-7827037.

**Registry No.** Tl-203, 14280-48-9; Tl-205, 14280-49-0;  $\text{TiNO}_3$ , 10102-45-1;  $\text{KNO}_3$ , 7757-79-1.

(38) Wyckoff, R. W. G. *Phys. Rev.* **1920**, *16*, 149.

(39) Kracek, F. C.; Posnjak, E.; Hendricks, S. B. *J. Am. Chem. Soc.* **1931**, *53*, 3339.

(40) Lindley, P. F.; Woodward, P. *J. Chem. Soc. A* **1966**, 123.